Vol 447|3 May 2007|doi:10.1038/nature05776

LETTERS

Direct measurement of antiferromagnetic domain fluctuations

O. G. Shpyrko[1], E. D. Isaacs[1,3], J. M. Logan[3], Yejun Feng[3], G. Aeppli[4], R. Jaramillo[3], H. C. Kim[3], T. F. Rosenbaum[3], P. Zschack[2], M. Sprung[2], S. Narayanan[2] & A. R. Sandy[2]

Measurements of magnetic noise emanating from ferromagnets owing to domain motion were first carried out nearly 100 years ago[1], and have underpinned much science and technology[2,3]. Antiferromagnets, which carry no net external magnetic dipole moment, yet have a periodic arrangement of the electron spins extending over macroscopic distances, should also display magnetic noise. However, this must be sampled at spatial wavelengths of the order of several interatomic spacings, rather than the macroscopic scales characteristic of ferromagnets. Here we present a direct measurement of the fluctuations in the nanometre-scale superstructure of spin- and charge-density waves associated with antiferromagnetism in elemental chromium. The technique used is X-ray photon correlation spectroscopy, where coherent X-ray diffraction produces a speckle pattern that serves as a 'fingerprint' of a particular magnetic domain configuration. The temporal evolution of the patterns corresponds to domain walls advancing and retreating over micrometre distances. This work demonstrates a useful measurement tool for antiferromagnetic domain wall engineering, but also reveals a fundamental finding about spin dynamics in the simplest antiferromagnet: although the domain wall motion is thermally activated at temperatures above 100 K, it is not so at lower temperatures, and indeed has a rate that saturates at a finite value—consistent with quantum fluctuations—on cooling below 40 K.

Because of scientific and technical interest in ferromagnetic domains, there has been substantial, long-standing work on magnetic noise in ferromagnets as a direct witness of domain motion. As antiferromagnets begin to find applications themselves—for example, as pinning layers in spintronics—there is a need for measurements of the noise associated with moving antiferromagnetic domains. Antiferromagnetic domain dynamics are also important because they are implicated in basic problems in condensed matter physics, such as high temperature superconductivity and 'heavy' fermions. Neutrons are an excellent non-local probe of antiferromagnetism and its dynamics[4]. However, a direct local probe of mesoscopic antiferromagnetic domain dynamics has not been hitherto available; this is because the magnetic dipole moments for antiferromagnets vanish on the scale of a nanometre, rendering the domain fluctuations responsible for noise essentially invisible to the direct magnetometer probes (for example, superconducting interference devices) that have been so successful for ferromagnets[5].

Chromium is a body-centred cubic (b.c.c.) metal with an antiferromagnetic state nearly described by the simple rule that the electrons surrounding each Cr atom have magnetization opposite to those on the nearest neighbour Cr atoms. What actually occurs is sinusoidal modulation of this elementary magnetic structure—called a spin

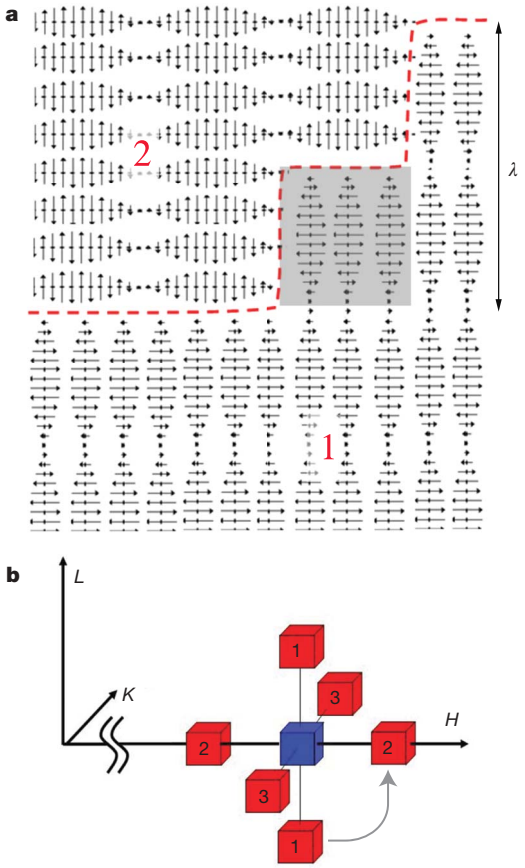

Figure 1 | Spin-density wave (SDW) domain wall in chromium. a, Schematic representation of the domain wall (red dashed line) separating two regions with perpendicular orientations of transverse SDW. The domain wall is shown to propagate along the weak nodal planes—where local magnetization approaches zero. Shaded region represents an elementary domain unit with volume $(\lambda/2)^3$, where λ is the SDW period, that can be thought of as a magnetic quantum dot in a cubic lattice of similar quantum dots. **b**, Reciprocal space configuration of the lattice [200] Bragg peak (blue) and six surrounding charge-density wave (CDW) satellites (red). *H*, *K* and *L* define fundamental axes of the reciprocal cubic lattice. Domains marked as 1 and 2 in **a** contribute to pairs of satellites marked 1 and 2 in **b**, respectively. A 90° rotation of SDW propagation vector within the shaded elementary volume of domain 1 would realign spins with domain 2, resulting in a shift of the domain wall and a transfer of scattering intensity from satellite pairs 1 to 2, marked with an arrow in **b**.

[1]Center for Nanoscale Materials, [2]Advanced Photon Source, Argonne National Laboratory, Argonne, Illinois 60439, USA. [3]James Franck Institute and Department of Physics, University of Chicago, Chicago, Illinois 60637, USA. [4]London Centre for Nanotechnology and Department of Physics and Astronomy, University College London, London WC1E 6BT, UK.

density wave (SDW), with wavelength $\lambda = 6$–8 nm—along one of the three equivalent cubic (100) directions. A single crystal chromium sample cooled below the Néel temperature, $T_N = 311$ K, spontaneously breaks (see Fig. 1) into three types of magnetic domains characterized by the three different choices for the SDW propagation direction (for a review of SDWs in Cr, see ref. 6). The SDW is accompanied by a charge density wave (CDW), a combination of both itinerant and ionic charge modulation.

X-ray microdiffraction reveals that the typical size of the SDW domains in bulk Cr samples is of the order of 1–30 μm (ref. 7). Fluctuations of domain walls at fixed temperature have been studied via random electrical telegraph noise in thin Cr films for temperatures above 140 K (ref. 8). Even though the measurements were done for mesoscopic samples, the effects on the electrical resistance (R) of the switching dynamics were small ($\delta R/R \approx 10^{-5}$) and the interpretation difficult because R is an indirect probe of the underlying SDW and CDW order.

We report the first direct observations of domain wall fluctuations in bulk Cr using X-ray photon correlation spectroscopy (XPCS), which overcomes the limitations of the classic bulk and laser probes in that it accesses directly the short wavelength structure associated with the SDW. A coherent beam illuminating a partially ordered system (in our case consisting of SDW/CDW domains) produces an interference pattern, also known as speckle[9,10]. Owing to the high sensitivity of speckle to minute changes in domain wall configuration, the time variation of the speckle pattern directly reveals the dynamics of domain structure. Figure 2a is a diagram of the experimental configuration, and Fig. 2b shows a speckle pattern of the (200) Bragg peak for the b.c.c. Cr lattice. Interference fringes arising from partial coherence of the X-ray beam are clearly seen in the image, as well as in the line scans (Fig. 2c). Incoherent diffraction would produce the gaussian-like profile represented by the black line in Fig. 2c. The lattice Bragg speckle pattern is static over 5 h, indicating the high level of stability for our instrumentation and the sample.

We turn next to the speckle pattern for the $[2-2\delta, 0, 0]$ CDW superlattice reflection, displayed for 17 K at a variety of times in Fig. 3b. The patterns in subsequent frames, separated by 1,000 s, grow increasingly dissimilar for longer time lags—patterns within frames collected more than 3,000 s apart appear completely uncorrelated. Thus, the CDW speckle evolves with a characteristic time of a few thousand seconds or less, much shorter than the >20,000 s relaxation time for the b.c.c. Bragg speckle of Fig. 2c. This indicates that the changes in the CDW speckle are indeed due to changes in the magnetic domain configuration, rather than some experimental artefact. For example, drift of the X-ray beam or the cryostat, motion of crystalline defects within the Cr sample, or any other effect not related to magnetic domain dynamics would inevitably cause changes in both the CDW and (200) Bragg speckle.

The spatial sensitivity of the speckle to domain motion is described by two distinct lengths: the first is $1/\Delta Q \approx 100$ Å, where $\Delta Q = 10^{-2}$ Å^{-1} is the total size of visible speckle pattern in reciprocal space (see Figs 2b, c and 3b) and represents the minimum size of domains with a visible impact on the speckle pattern. The second is the domain wall displacement necessary to produce a speckle pattern that is highly dissimilar (or uncorrelated) to the original one. A combination of X-ray microdiffraction images of domain configurations and speckle simulations indicate that this second length is 1 μm (see Methods and Supplementary Information).

Beyond revealing that domain walls are moving by distances of the order of 1 μm, the data provide several other important quantities. For example, we can evaluate the autocorrelation function, $g_2(t)$:

$$g_2(t) = \frac{\langle I(\tau)I(\tau+t)\rangle_\tau}{\langle I(\tau)\rangle_\tau^2} = 1 + A|F(\mathbf{Q},t)|^2 \qquad (1)$$

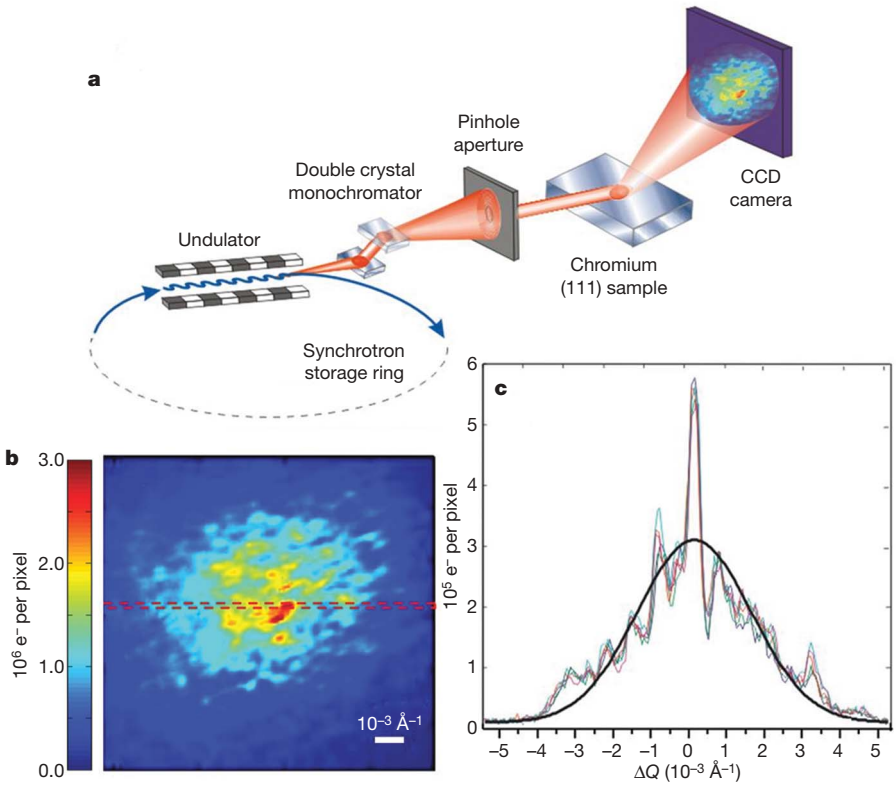

Figure 2 | X-ray speckle measurements. **a**, Diagram of the experimental set-up. **b**, CCD image of the X-ray speckle observed for the [200] lattice Bragg reflection. **c**, Intensity distribution for a line scan across the region between the dashed lines in **b**. Five differently coloured and nearly identical lines represent line scans of the portion of speckle pattern shown between the red dashed lines in **b**, taken one hour apart. The black line is a simulated statistically averaged gaussian profile, expected for a completely incoherent beam.

where $I(\tau)$ and $I(\tau + t)$ are the intensities in a given pixel for frames taken at times τ and $\tau + t$ respectively, $F(\mathbf{Q},t)$ is the intermediate scattering function, A describes the beam coherence[9,10], and the averaging is performed over times τ and pixels corresponding to wavevector $\mathbf{Q}$. Figure 3a shows $|F(\mathbf{Q},t)|^2$ for several temperatures calculated from the CDW speckle at $\mathbf{Q} = [2-2\delta, 0, 0]$. For large time delays the speckle patterns become uncorrelated, resulting in $g_2(t) = 1$, corresponding to $|F(\mathbf{Q},t)|^2 = 0$. The dynamics are strongly temperature-dependent: on cooling, the domain fluctuation times increase by nearly two decades. Surprisingly, below 40 K the times remain finite, rather than diverging as expected for thermally driven fluctuations.

Two distinct fluctuation timescales are visible in most data sets presented in Fig. 3a. The measured $|F(\mathbf{Q},t)|$ was therefore modelled by a double exponential form:

$$|F(\mathbf{Q},t)| = a\exp\left(-(t/\tau_F)^{\beta}\right) + (1-a)\exp\left(-(t/\tau_S)^{\beta}\right) \quad (2)$$

where τ_F and τ_S represent the characteristic fast and slow fluctuation timescales, respectively. A small value of $a = 0.03$–0.10 indicates that the time dependence of $|F(\mathbf{Q},t)|$ is mainly due to slow fluctuations. The value of the stretching exponent β was found to be greater than 1, manifested by the 'compressed' shape of the $|F(\mathbf{Q},t)|$. Compressed exponential relaxation has been observed for a variety of soft matter systems undergoing 'jamming' transitions, which result in arrested, solid-like collective dynamics[11–13] with $\beta > 1$, instead of liquid-like fluctuations with $\beta \leq 1$. Extended to our system, this points to elastically coupled dynamics between blocks of spins, similar to elastic collective depinning dynamics observed in CDW conductors[14], an observation also consistent with the weakly pinned nature of SDW/CDW domains[15–17]. Furthermore, the fit value of β at $T < 100$ K is approximately 1.5 (Fig. 4, left inset), a universal value for dynamics of soft condensed matter systems in a jammed state[18].

Figure 4 shows the T-dependence of the slow relaxation times τ_S obtained from fits to autocorrelation functions in Fig. 3a. The 20% uncertainty in fitting parameters τ_S arises primarily from counting statistics of the autocorrelation function $g_2(t)$ (see Supplementary Information). Standard thermal activation ($\tau_S^{-1} = f_o\exp(-\Delta E/k_BT)$, blue line) with a single attempt frequency f_o and activation barrier $\Delta E/k_B = 240 \pm 50$ K accounts for the data at high T. The thermal picture fails spectacularly at low temperature for $T < 40$ K, and a switching mechanism which is temperature-independent in this range is required. The simplest possibility is that switching between low-energy domain wall configurations occurs via quantum tunnelling, rather than classical thermal activation (Fig. 4, right inset). A fit to the data that combines a thermally activated model and a quantum tunnelling contribution represented by a temperature-independent residence time τ_{QT}, $\tau_S^{-1} = \tau_{QT}^{-1} + \tau_R^{-1}\exp(-\Delta E/k_BT)$ is shown by the red solid line in Fig. 4 for $\tau_{QT} = 5{,}000$ s and $\tau_R = 15$ s (confidence limits obtained from the fits are $\tau_{QT} = 5{,}000 \pm 1{,}000$ s and $\tau_R = 4$–60 s). In analogy with α and β relaxation observed in glasses, supercooled liquids and jammed soft matter systems, faster fluctuations represent local relaxation, while slower fluctuations are due to collective relaxation modes.

The relaxation times observed here are similar to those associated with magnetization switching in ferromagnets first observed by Barkhausen[1] and studied since then in systems ranging from bulk materials to magnetic molecules[5,19–22]. Antiferromagnets have more complex order than ferromagnets because they break translation as well as spin rotation invariance, which has forced us to formulate a very crude physical picture in order to understand our data at a semiquantitative level. We start with the realization that to minimize the very large exchange energy (>0.4 eV)[23,24] associated with domain walls, it is clearly advantageous for the domain walls to lie on the nodal planes[25] (where the spin polarization vanishes). Such an assumption is further supported by the previously observed preference for the formation of SDW nodes at Fe/Cr interfaces[26]. This implies that the fundamental switching unit (grey shaded region in Fig. 1a) has volume $V_S \approx (\lambda/2)^3$, where λ is the underlying period of the SDW. In the simplest gaussian model where underlying units are switching randomly at typical times τ_U, we would conclude that the switching time for a volume of $V = 1\ \mu m^3$ would be $(V/V_S)^2\tau_U$. Using our experimental value for the attempt frequency τ_R^{-1}, we therefore

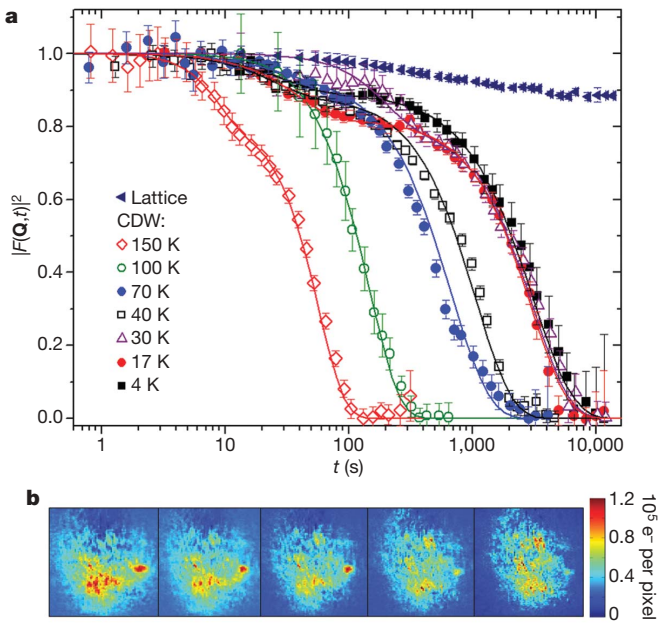

Figure 3 | Autocorrelation of speckle images. **a**, Intensity autocorrelation data for the [200] lattice Bragg peak, as well as for the CDW superlattice $[2-2\delta, 0, 0]$ peak, at temperatures T (in K) 150, 100, 70, 40, 30, 17 and 4. Error bars, standard deviation calculated for a region of interest within the CCD typically containing $n = 4 \times 10^4$ pixels. Two distinct timescales are clearly present in the CDW autocorrelation function. Solid lines represent theoretical fits to the data. See text for further details. **b**, Time sequence of CDW speckle pattern evolution at 17 K. Subsequent images are taken 1,000 s apart; each image is 10^{-2} Å$^{-1} \times 10^{-2}$ Å^{-1}.

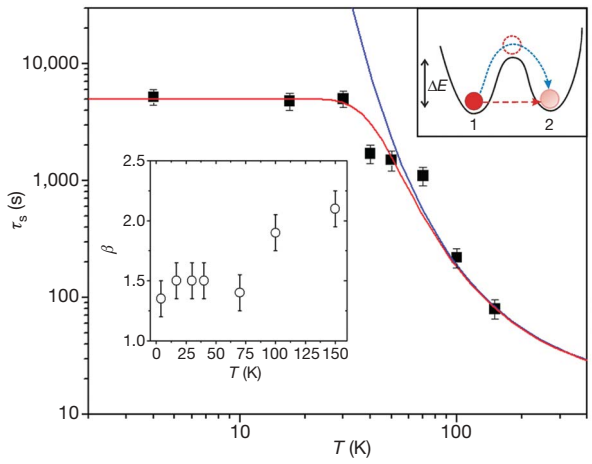

Figure 4 | Temperature-dependent domain wall dynamics. Main plot, characteristic slow fluctuation timescale, τ_S, obtained from fits to autocorrelation function data shown in Fig. 3a, compared to a classical Arrhenius model (blue line) and a model that also includes a temperature-independent switching rate term (red line). Right inset, potential energy surface including thermally activated (blue dashed line) and quantum tunnelling (red dashed line) mechanisms of the transition between the two low energy domain configurations 1 and 2 (see Fig. 1 for an example involving elementary switching volume) separated by energy barrier ΔE. Left inset, values of stretching exponent β for various temperatures. Error bars for τ_S and β represent the range of parameters obtained from fitting the autocorrelation data in Fig. 3.

obtain $\tau_U^{-1} = 36\,\mathrm{THz} = 140\,\mathrm{meV}$ as the attempt frequency for rotating an entire unit. This is an electronic energy scale, and could therefore be derived from the hopping of electrons across the domain wall; such electrons (also important in electrical noise measurements[8]) are, after all, responsible for the current fluctuations that sample the possibility of rotating the Fermi surface of a 'quantum dot' with the fundamental unit volume V_S. The tunnelling degree of freedom, which involves rotating the Fermi surface and its proxy, the **Q** vector, can be considered a spherical rotor in a potential with minima along the cubic *x*, *y* and *z* directions. Our measured barrier height ΔE is not far from the Néel temperature, which allows us to think of the antiferromagnetic phase transition as occurring when *Q*-domain walls become unstable to thermal fluctuations. The barriers between the potential minima could also be identified by magnetic neutron scattering, such as that performed for $Cr_{0.95}V_{0.05}$ (ref. 27). This underscores the fundamental complementary nature of the XPCS measurements of the dynamics as measured in the time domain, and dynamics measured by neutrons in the frequency domain.

In the simplest Wentzel-Kramers-Brillouin (WKB) approximation (see, for example, ref. 22), the dimensionless ratio τ_R/τ_{QT} is equal to $\exp(-S/\hbar)$, where $S = \sqrt{I\Delta E}$ is the tunnelling action and I is the moment of inertia of a single rotor. Because the underlying attempt frequencies and their rescaling to account for observable effects in the X-ray experiment are the same for both incoherent quantum and classical processes, all of the detail—invoking multiple rotors—of the last paragraph drops out, and S characterizes a single rotor. We can therefore calculate the moment of inertia I of the quantum rotor using the measured parameters τ_{QT}, τ_R and the barrier height $\Delta E = 20\,\mathrm{meV}$ obtained from the Arrhenius regime. The result is $I = 100 m_e\,\mathrm{nm}^2$, which, assuming a cube of uniform density distributed over the $(\lambda/2)^3$ volume of the fundamental unit, corresponds to 0.1 electron mass (m_e) per chromium unit cell. This remarkable result, derived only from our data and the simple physical picture of Fig. 1, is consistent with Hall effect data[28,29] showing that the SDW is associated with the loss of a similar number of carriers, which of course must be moved with the rotors when there is a switching event.

We have introduced the direct measurement of noise spectra in antiferromagnets. Our experiments access local mesoscale spin dynamics with just a few domain walls in the illuminated volume, an advantage over non-local experimental probes that cannot be easily applied to macroscopic or bulk structures. The key finding is that even in bulk samples, and at temperatures very low compared to the Néel temperature, domain walls can be visibly unstable on timescales of fractions of an hour. What this means is that the stability of antiferromagnetism needs to be engineered—for example, by insertion of appropriate pinning centres—into devices that exploit it. This will become even more important for nanoscale spintronics that include antiferromagnetic elements. Beyond the obvious advantages for magnetic engineering of now having a technique with which antiferromagnetic domain fluctuations can be readily assessed, we foresee tremendous opportunities in areas such as the science of antiferromagnetic nanoparticles.

METHODS

Experiments were carried out at beamlines 33-ID and 8-ID of the Advanced Photon Source, Argonne National Laboratory. The undulator-generated X-rays are monochromatized by a Si(111) crystal at an energy $E = 7.35\,\mathrm{keV}$ (wavelength 1.686 Å). A 10 μm pinhole aperture or 10 μm (horizontally) by 40 μm (vertically) slits placed 5 cm upstream from the sample selected the partially coherent portion of the X-ray beam with a resulting coherence fraction $A \approx 0.07$–0.18. A high purity Cr(111) wafer (Alfa Aesar) was used to ensure a roughly equal population of domains along the three fundamental cubic axes. The sample was mounted inside a low-drift He flow cryostat, with thermal shielding provided by 600-μm-thick Be dome. Speckle patterns were recorded with a Princeton Instruments PI-LCX 1300 deep depletion X-ray CCD camera (1,340 × 1,300 pixel array, with 20 μm × 20 μm pixel size), located 150 cm from the sample in reflection geometry.

Received 4 December 2006; accepted 20 March 2007.

1. Barkhausen, H. Zwei mit Hilfe der Neuen Verstärker entdeckte Erscheinungen. *Phys. Z.* **20,** 401–403 (1919).
2. Weissman, M. B. Low frequency noise as a tool to study disordered materials. *Annu. Rev. Mater. Sci.* **26,** 395–429 (1996).
3. Sethna, J. P., Dahmen, K. A. & Myers, C. R. Crackling noise. *Nature* **410,** 242–250 (2001).
4. Shull, C. G. & Brockhouse, B. N. in *Nobel Lectures, Physics 1991–1995* (ed. Ekspong, G.) 107–154 (World Scientific, Singapore, 1997).
5. Vitale, S., Cavalieri, A., Cerdonio, M., Maraner, A. & Prodi, G. A. Thermal equilibrium noise with 1/f spectrum in a ferromagnetic alloy: Anomalous temperature dependence. *J. Appl. Phys.* **76,** 6332–6334 (1994).
6. Fawcett, E. Spin-density-wave antiferromagnetism in chromium. *Rev. Mod. Phys.* **60,** 209–283 (1988).
7. Evans, P. G., Isaacs, E. D., Aeppli, G., Cai, Z.-H. & Lai, B. X-ray microdiffraction image of antiferromagnetic domain evolution in chromium. *Science* **295,** 1042–1045 (2002).
8. Michel, R. P., Israeloff, N. E., Weissman, M. B., Dura, J. A. & Flynn, C. P. Electrical-noise measurements on chromium films. *Phys. Rev. B* **44,** 7413–7425 (1991).
9. Sutton, M., Mochrie, S. G. J., Greytak, T., Nagler, S. E. & Berman, L. E. Observation of speckle by diffraction with coherent X-rays. *Nature* **352,** 608–610 (1991).
10. Sutton, M. in *Third-Generation Hard X-Ray Synchrotron Radiation Sources: Source Properties, Optics, and Experimental Techniques* (ed. Mills, D.) 101–123 (Wiley & Sons, New York, 2002).
11. Cipelletti, L., Manley, S., Ball, R. C. & Weitz, D. A. Universal aging features in the restructuring of fractal colloidal gels. *Phys. Rev. Lett.* **84,** 2275–2278 (2000).
12. Bandyopadhyay, R. *et al.* Evolution of particle-scale dynamics in an aging clay suspension. *Phys. Rev. Lett.* **93,** 228302 (2004).
13. Falus, P., Borthwick, M. A., Narayanan, S., Sandy, A. R. & Mochrie, S. G. J. Crossover from stretched to compressed exponential relaxations in a polymer-based sponge phase. *Phys. Rev. Lett.* **97,** 066102 (2006).
14. Lemay, S. G., Thorne, R. E., Li, Y. & Brock, J. D. Temporally ordered collective creep and dynamic transition in the charge-density-wave conductor $NbSe_3$. *Phys. Rev. Lett.* **83,** 2793–2796 (1999).
15. Fukuyama, H. & Lee, P. A. Dynamics of the charge-density wave. I. Impurity pinning in a single chain. *Phys. Rev. B* **17,** 535–541 (1978).
16. Fukuyama, H. & Lee, P. A. Dynamics of the charge-density wave. II. Long-range Coulomb effects in an array of chains. *Phys. Rev. B* **17,** 542–548 (1978).
17. Littlewood, P. B. & Rice, T. M. Metastability of the *Q* vector of pinned charge- and spin-density waves. *Phys. Rev. Lett.* **48,** 44–47 (1982).
18. Cipelletti, L. *et al.* Universal non-diffusive slow dynamics in aging soft matter. *Faraday Discuss.* **123,** 237–251 (2003).
19. Chudnovsky, E. M. & Tejada, J. *Macroscopic Quantum Tunneling of the Magnetic Moment* (Cambridge University Press, Cambridge, UK, 1998).
20. Barbara, B. *et al.* Quantum tunneling in magnetic systems of various sizes. *J. Appl. Phys.* **73,** 6703–6706 (1993).
21. Wernsdorfer, W. Classical and quantum magnetization reversal studied in nanometer-sized particles and clusters. *Adv. Chem. Phys.* **118,** 99–190 (2001).
22. Brooke, J., Rosenbaum, T. F. & Aeppli, G. Tunable quantum tunnelling of magnetic domain walls. *Nature* **413,** 610–613 (2001).
23. Fenton, E. W. & Leavens, C. R. The spin density wave in chromium. *J. Phys. F* **10,** 1853–1878 (1980).
24. Fenton, E. W. Domains in the spin-density-wave phases of chromium. *Phys. Rev. Lett.* **45,** 736–739 (1980).
25. Michel, R. P., Weissman, M. B., Ritley, K., Huang, J. C. & Flynn, C. P. Suppression of polarization fluctuations in chromium alloys with commensurate spin-density waves. *Phys. Rev. B* **47,** 3442–3445 (1993).
26. Fullerton, E. E., Bader, S. D. & Robertson, J. L. Spin-density-wave antiferromagnetism of Cr in Fe/Cr(001) superlattices. *Phys. Rev. Lett.* **77,** 1382–1385 (1996).
27. Hayden, S. M., Doubble, R., Aeppli, G., Perring, T. G. & Fawcett, E. Strongly enhanced magnetic excitations near the quantum critical point of $Cr_{1-x}V_x$ and why strong exchange enhancement need not imply heavy fermion behavior. *Phys. Rev. Lett.* **84,** 999–1002 (2000).
28. Lee, M., Husmann, A., Rosenbaum, T. F. & Aeppli, G. High resolution study of magnetic ordering at absolute zero. *Phys. Rev. Lett.* **92,** 187201 (2004).
29. Yeh, A. *et al.* Quantum phase transition in a common metal. *Nature* **419,** 459–462 (2002).

Supplementary Information is linked to the online version of the paper at www.nature.com/nature.

Acknowledgements Use of the Center for Nanoscale Materials and Advanced Photon Source was supported by the US Department of Energy, Office of Science, Office of Basic Energy Sciences. Work at the University of Chicago was supported by the National Science Foundation, while that in London was funded by a Royal Society Wolfson Research Merit Award and the Basic Technologies programme of RCUK.

Author Information Reprints and permissions information is available at www.nature.com/reprints. The authors declare no competing financial interests. Correspondence and requests for materials should be addressed to O.G.S. (oshpyrko@anl.gov).